| | |
|---|---|
| **Preprint Title** | Synergistic effect of hybrid graphene oxide-aluminum dihydric tripolyphosphate in epoxy-based anticorrosive coatings |
| **Authors** | Weiqiang Song, Xiaohua Liu, Qingsong Zhu and Yuxiang Zhang |
| **Publication Date** | 15 Jan 2020 |
| **Article Type** | Full Research Paper |
| **ORCID® iDs** | Weiqiang Song - https://orcid.org/0000-0003-4811-5766 |

# Synergistic effect of hybrid graphene oxide-aluminum dihydric tripolyphosphate in epoxy- based anticorrosive coatings

*Weiqiang Song [1,*], Xiaohua Liu [1], Qingsong Zhu [1, 2], Yuxiang Zhang [3]*

*([1] School of Materials Science and Engineering, Henan University of Technology, Zhengzhou 450001, PR China)*
*([2] College of Materials Science and Engineering, The Key Laboratory of Material Processing and Mold of Ministry of Education, Zhengzhou University, Zhengzhou 450001, PR China)*
*([3] School of Energy and Power Engineering, Zhengzhou University of Light Industry, Zhengzhou 450002, PR China)*
[*] Corresponding author: Weiqiang Song
E-mail: weiqiang_song@haut.edu.cn
Post address: 100 Lianhua Road, Zhengzhou Hi-tech Development Zone, 450001, P. R. China
Telephone: 086+18623719057

**ABSTRACT**

ADTP-GO hybrid was prepared from multi-layered aluminum dihydric tripolyphosphate (ADTP) and flake-shaped graphene oxide (GO) by a coupling method using (3-aminopropyl) triethoxysilane (ASi) as the coupling agent. Characterization analyses of the hybrid were performed by FT-IR, XRD and SEM. The effect of incorporating 2wt% ADTP-GO hybrid on corrosion inhibition performance of epoxy coating was evaluated in 3.5wt.% NaCl aqueous solution by using Tafel and electrochemical impedance spectroscopy (EIS) analysis. For comparison, the effects of ADTP and GO, alone and in combination without coupling treatment were also evaluated. FT-IR and XRD showed the presence of the chemical interaction between ADTP and GO in ADTP-GO hybrid. SEM indicated that GO was spread on the surface of ADTP layers in the hybrid. Tafel and EIS data indicated that the hybrid displayed an anti-corrosion performance superior to ADTP/GO blend without coupling treatment. The superiority was attributed to the stronger synergetic effect of ADTP and GO in ADTP-GO hybrid than in ADTP/GO blend. Additionally, epoxy/ADTP/GO coating was better than pure epoxy, epoxy/ADTP, and epoxy/GO coatings in the anti-corrosion performance on mild steel. It seems that the combination of ADTP and GO produced synergistic effect, and the synergistic effect was more obvious after chemical coupling.

**Keywords:** graphene oxide; aluminum dihydric tripolyphosphate; layered hybrid; epoxy coating; anticorrosion

## ■ INTRODUCTION

Organic coatings are the single most widely applied method for corrosion protection of metallic materials, especially metal products made from steel or aluminum, due to their low cost, versatility, decoration aesthetics and effective protections. Protective organic coatings normally consist of a continuous polymeric phase known as the “binder” and various discontinuous solid functional additives, commonly known as “pigments” that are contained within the continuous phase.[1] Accordingly, the polymeric binder not only acts as a physical barrier layer to control the ingress of deleterious species, but also serves as a reservoir for corrosion inhibitors to aid the metallic substrate surface in resisting attack by aggressive species such as oxygen, water and electrolyte. In this regard, epoxy resin is widely employed as the polymeric binder due to its excellent chemical stability, outstanding corrosion resistance, strong adhesion/affinity to heterogeneous materials.[2, 3]

Nonetheless, the successful application of anti-corrosive epoxy coatings was hampered due to

intrinsic characteristics and external hazards. [4] Epoxy resins are inherently brittle and therefore show poor resistance to the initiation and propagation of cracks. Such processes and the resulting stress cause localized defects in the coatings and do harm to their appearance and mechanical strength. Additionally, micropores are inevitably produced in their structure due to solvent evaporation and the mixed gas escaping.[5] The defects and micropores can act as pathways accelerating the ingress of water, oxygen and other aggressive species onto the metallic substrate, resulting in their localized corrosion.[6]

Although corrosion protection theories and failure modes of anti-corrosion organic coatings are not fully understood due to complicated interactions in the coating-metal-environment system, it is still widely agreed that the barrier nature of polymeric materials to the passage of aggressive species, such as oxygen, water, electrolyte, is responsible for corrosion protection.[7] The barrier performance of epoxy coatings can be enhanced by the incorporation of a inorganic powder pigment, which is miscible with the epoxy resin and easy to disperse and keep stable in the resin, by decreasing the porosity in the coatings. The incorporation of a pigment into epoxy resins additionally offers solutions to barrier performance, since the tiny particles dispersed in coatings can fill cavities and cause crack bridging, crack deflection and crack bowing. Tiny particles tend to occupy small hole defects and act as a bridge interconnecting more molecules, resulting in a reduced total free volume as well as an increase in the cross-linking density.[8-10] A layered pigment offers additional solution to barrier performance by zigzagging the diffusion path for aggressive species.[11] Layered pigments such as exfoliated clay and layered double hydroxides have effectively increased the diffusion pathways of water and destructive ions, thereby enhancing the protection performance of the coatings.[12] There has been significant recent interest in the development of graphene oxide (GO) as a possible additive to epoxy coatings because of its typical two-dimensional lamellar structure. GO remarkably improved the corrosion resistance of organic coatings by extending the path of corroding agents in the coatings to reach to the metal/coating interface and then enhancing the barrier properties of polymer matrix.[13-15]

In many cases, the anti-corrosion coatings rely on an inhibition mechanism rather than a resistive or barrier mechanism for their performance in the field, so inhibitive anticorrosive pigments have been widely used in coatings.[16, 17] Some toxic inorganic pigments containing chromium, lead, cadmium and so on, like chrome yellow, zinc yellow and lead red, were widely used in history because of their excellent corrosion resistance, but not generally considered inhibitors because of their toxicity and corresponding legislative restrictions. New generations of pigments have been suggested and used widely as environmentally friendly alternatives, although they do not quite match the high efficiency of lead or chromium (VI) compounds.[17,18] Recent efforts to increase their efficiency have mainly been focused on the alternatives and GO in combination as inhibitors in coatings.[19-21]

Among alternative pigments to lead- and chromate-containing pigments, aluminum dihydric tri-polyphosphate (ADTP) as a completely non-toxic one is preferred for preparation of special anticorrosive coatings, such as the interior coatings of metal cans. Interestingly, ADTP has a multi-layered configuration,[22] which is similar to flaky GO in a way. In this communication, two approaches were introduced to combine ADTP and GO, i.e., physical blending and chemical coupling. The anti-corrosion performance of the pigments in epoxy coatings on mild steel was evaluated comparatively.

## ■ EXPERIMENTAL SECTION

**Materials.** Natural flake graphite was purchased from Angxing Technology Co., Ltd. (3-aminopropyl) triethoxysilane (ASi) was purchased from Zhengzhou Alfachem Co., Ltd. Epoxy resin emulsion (CYDW-112W50, epoxy equivalent in the range of 1200 to 1850 g/mol) and a modified alicyclic amine (CYDHD-W280, amine value in the range of 260 to 320 mg KOH/g) as the curing agent were supplied by Yueyang Baling Petrochemical CO., Ltd. All the other chemicals were of analytical reagent grade and obtained from Tianjin Kemiou Chemical Reagent Co., Ltd.

**Synthesis of ADTP.** In a typical procedure, aluminum hydroxide slurry and phosphoric acid solution (mole ratio of $P_2O_5$ / $Al_2O_3$ is 3:1) were mixed at 90° C in a container. The container was stirred at 100° C for 1.5 hours and the mixture turned into translucent viscous slurry. The slurry was immediately placed into a reacting furnace set at 310° C. After reacting for 10 hours, the obtained solid was taken out of the furnace and immersed into distilled water. After hydration reaction, the product was treated by dehydration drying and further crushing. Although X-ray diffraction (XRD) studies revealed a coexistence of two main structural phases of ADTP and $AlPO_4$ in the product, the product was not further separated and purified. The reaction scheme of the formation of ADTP is shown as following.

$$Al_2O_3 + 3H_3PO_4 \rightarrow Al(H_2PO_4)_3$$
$$3Al(H_2PO_4)_3 \rightarrow AlH_2P_3O_{10}\ (\text{Type I}) + 2HO$$
$$AlH_2P_3O_{10}\ (\text{Type I}) + 2H_2O \rightarrow AlH_2P_3O_{10} \cdot 2H_2\ O$$

**Synthesis of GO.** GO was made by the Hummers method. 98% $H_2SO_4$ (115 ml) and natural graphite (5 g, purchased from Angxing Technology Co., Ltd.) were added into a 1000 ml beaker and magnetically stirred for 2 hours. Then, $KMnO_4$ (15 g) and $NaNO_3$ (2.5 g) were introduced within 2 hours at 0° C (ice bath) before the mixture in the beaker was heated at 35° C for 2 hours. Subsequently, the temperature was raised to 95° C and 230 ml of distilled water was dropped into the mixture. After that, 30% $H_2O_2$ (5 ml) and distilled water (600 ml) were added into the mixture. The mixture was centrifugally washed three times with 10% HCl solution at the rotary speed of 4000 r/min, and again centrifugally washed three times with distilled water at the rotary speed of 8000 r/min. The final brown-black viscous jelly was collected and dried at 60° C for 24 hours. The stably dispersed solution of GO was obtained by ultrasonically dispersing the resulted filter cake in distilled water for 20 min.

**Preparation of ADTP/GO blend.** ADTP and GO were ultrasonically dispersed into DMF solvents, respectively, and then mixed in a three-necked flask. The mixture was heated to 105° C in an oil bath with stirring at 1000 r/min, and kept at the temperature for 5 h. After that, the mixture was centrifuged at 4000 r/min and the precipitate was washed with ethanol. Subsequently, the precipitate was dried at 60° C for 24 hours. After grinding, the resulting powder was used as ADTP/GO blend.

**Preparation of ADTP-GO hybrid.** The schematic illustration of the preparation process of ADTP-GO hybrid is presented in Figure 1.

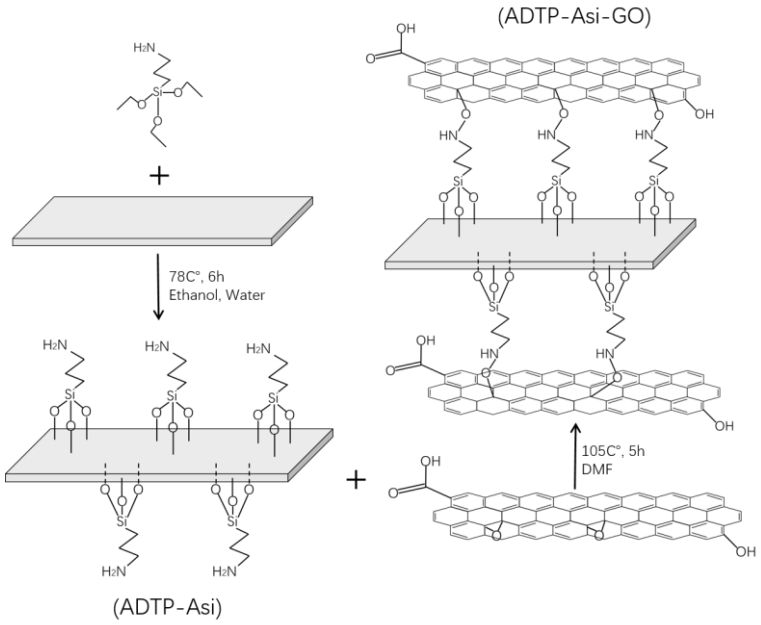


**Figure 1.** Reaction scheme of the formation of ADTP-GO nanohybrid

Firstly, ADTP was modified by a silane coupling agent with amino group. ADTP was mixed with ASi and distilled water in the weight ratio of 1:1:5 in ethanol under magnetic stirring. The mixture was heated to the reflux temperature and kept at this temperature for 6 hours. The product was washed with ethanol for several times to remove excessive ASi and subsequently dried at 60 °C for 24 hours. After grinding, ADTP modified by ASi was obtained, and labeled as ADTP-ASi.

Secondly, ADTP and GO were connected with ASi. The aforementioned ADTP-ASi and GO were ultrasonically dispersed into DMF solvents, respectively, and then mixed in a three-necked flask. The mixture was heated to 105 °C in an oil bath. After stirring at 1000 r/min for 5 hours, the mixture was centrifuged at 4000 r/min. The precipitate was collected and washed with ethanol. Subsequently, the precipitate was grinded after drying. The resulting powder was used as ADTP-GO hybrid.

**Preparation and Application of Composite Coatings.** Each of 5 pigment types (no pigment, ADTP, GO, ADTP/GO blend, and ADTP-GO hybrid) was dispersed into distilled water at 2wt.% and stirred by using a high-speed mixer at 2000 r/min for 2h. Subsequently, the epoxy resin emulsion was added into the obtained suspension solution and stirred at 1000 r/min for 30 min. After that, the curing agent was introduced into the mixture and stirred for 5 min. The finally obtained mixture was used as an epoxy coating.

Mild steel panels (120×50×0.28 mm) were treated by mechanical cleaning (polishing), degreasing in an acetone solution and rinsing with distilled water. The above obtained coating was applied on the panels by brush. The coating films were precured at room temperature for 24 hours then cured at 120 °C for 2 hours. The obtained solid films had a uniform thickness of about 60 μm, and were named as pure epoxy coating, epoxy/ADTP, epoxy/GO, epoxy/ADTP/GO and epoxy/ADTP-GO, respectively. Figure 2 exhibits the preparation process of epoxy resin-based coatings.

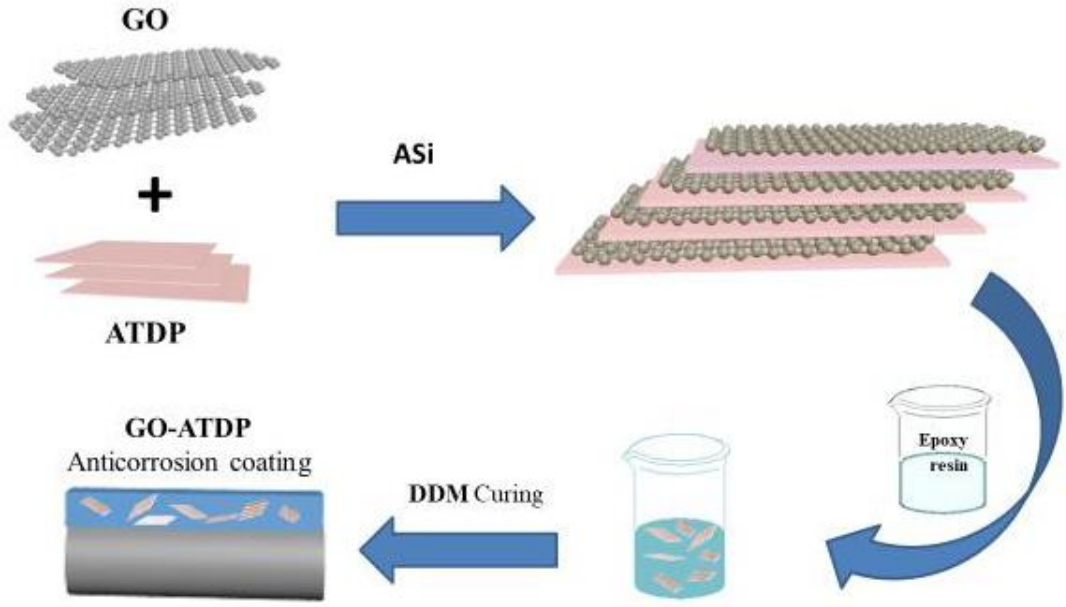


**Figure 2.** Preparation process of epoxy/ADTP-GO coating

**Characterization.** Infrared absorption spectra were recorded using Fourier infrared spectrometer (FTIR; Prestige-21), and the wavenumber range from 4000cm$^{-1}$ to 400cm$^{-1}$. The crystalline structure and composition of ADTP in powder form were analyzed by an X-ray diffractometer (XRD; Bruker D8 Advance) with monochromatized copper target *K*□ radiation (□= 0.154nm) at 40kV and 35mA, and the 2$\theta$ diffraction angle scanning range from 5° to 40°. The structure and composition of other as-products in powder form were analyzed by an X-ray diffractometer (Bruker D8 Discover) at 50kV and 1000μA and the 2$\theta$ diffraction angle scanning range from 2.5° to 32°.

Morphologies of the as-prepared pigments and coatings' fracture surface was observed by using scanning electron microscopy (SEM). An Inspect F50 Scanning Electron Microscope was run at an accelerating voltage of 20kV and an 18mm working distance. The fracture surface of the cured layer of the abovementioned epoxy coatings was also observed by using the same microscopy.

**Electrochemical Measurements.** Electrochemical measurements were conducted in RST5200F electrochemical working instrument (Zhengzhou shiruisi Instrument Technology Co., Ltd.) with a conventional three-electrode configuration. The electrochemical cell with Ag/AgCl reference electrode (RE), the aforementioned panels with cured film as the working electrode (WE) and platinum counter electrode (CE) was used to run the tests. The working electrode had a geometrical area of 1cm$^2$. The aforementioned extracts were used as the working solutions. The polarization curves were recorded at a scan rate of 1mVs$^{-1}$. Electrochemical impedance spectroscopy (EIS) measurements were carried out in the frequency range of $10^5$Hz to $10^{-2}$Hz, using perturbation amplitude of 5mV around the open circuit potential.

## ■ RESULTS AND DISCUSSION

**XRD Analysis.** XRD spectrum of the prepared ADTP is presented in Figure 3. The major peaks were assigned to $AlPO_4$ (JCPDS 45-0177 and 10-0423) and $AlH_2P_3O_{10}\cdot 2H_2O$ (JCPDS 31-0017), which indicated the ADTP was a composite of $AlH_2P_3O_{10}\cdot 2H_2O$ and $AlPO_4$. The strong diffraction peak at 2$\theta$=11.16° was attributed to $AlH_2P_3O_{10}\cdot 2H_2O$, and the corresponding value of *d* (*d*=$\lambda$/2sin$\theta$) was 7.947×10$^{-10}$ m. $AlH_2P_3O_{10}\cdot 2H_2O$ had a multilayered configuration with the terminal hydroxyl

groups connecting to $PO_4$ units. The hydroxyl groups protrude into the interlamellar region and formed hydrogen bonds with the interlamellar water molecules which in turn held the layers and structure together.[22]

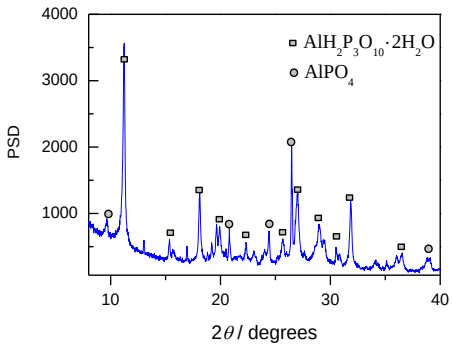


**Figure 3.** XRD spectrum of the prepared ADTP

XRD spectra of the prepared GO, ADTP-GO, and the natural flake graphite used in this study were presented in Figure 4. A sharp peak appeared at $2\theta$ nearly equal to 10.95°, corresponding to an interlayer spacing of 0.83nm, which corresponded to the characteristic diffraction peak of GO. Graphite had a very sharp and strong diffraction peak near $2\theta$ equal to about 26.16°, that is, the diffraction peak of graphite (002) surface. In addition, the sharp and strong diffraction peak at 5.84° indicated that the raw graphite had good lamellar structure. After graphite was oxidized, the diffraction peak of graphite (002) surface disappeared, which indicated that the crystal form of graphite was destroyed and a new crystal structure was formed. Particularly, the sharp peak revealed that GO sheets exhibited a close-packed layered and highly ordered structure. For ADTP-GO, there was an emergence of a sharp around at $2\theta$ nearly equal to 4.34°, corresponding to an increased interlayer spacing of 2.03nm, which implies that the formation of ADTP structure was transformed by ASi.

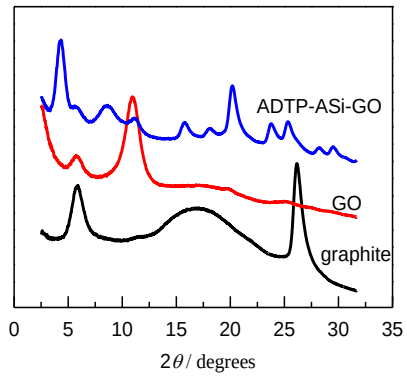


**Figure 4.** XRD spectra of GO sheets, ADTP-GO and graphite

**FTIR Analysis.** FTIR spectra of the involved products are presented in Figure 5. Absorption bands at 3595$cm^{-1}$ and 3521$cm^{-1}$ were due to asymmetric and symmetrical stretching vibrations of POH in $AlH_2P_3O_{10}·2H_2O$, respectively. A set of absorption bands in the range of 1250 to 950$cm^{-1}$ were due to P-O vibration absorptions. Bands at 1057$cm^{-1}$ and 986$cm^{-1}$ were due to strong characteristic vibration absorptions of $PO_4$ in $AlPO_4$ and $P_3O_{10}$ in $AlH_2P_3O_{10}·2H_2O$, respectively.

The bands around at 1247 and 1057$cm^{-1}$ in ADTP spectrum shifted to 1226 and 1029 $cm^{-1}$ in ADTP-ASi and ADTP-GO, respectively, which indicated the presence of chemical connection

between ADTP and ASi. The band at 811cm-1 hardly shifted in ADTP-ASi and ADTP/GO while it shifted slightly to 808cm$^{-1}$ in ADTP-GO. The band at 986cm$^{-1}$ in ADTP spectrum shifted to 969, 972 and 976cm$^{-1}$ in ADTP-GO, ADTP-ASi and ADTP/GO spectra, respectively. Significant changes in wave numbers of absorption bands after modification indicate that ADTP and ASi were chemically bonded rather than simply mixed.

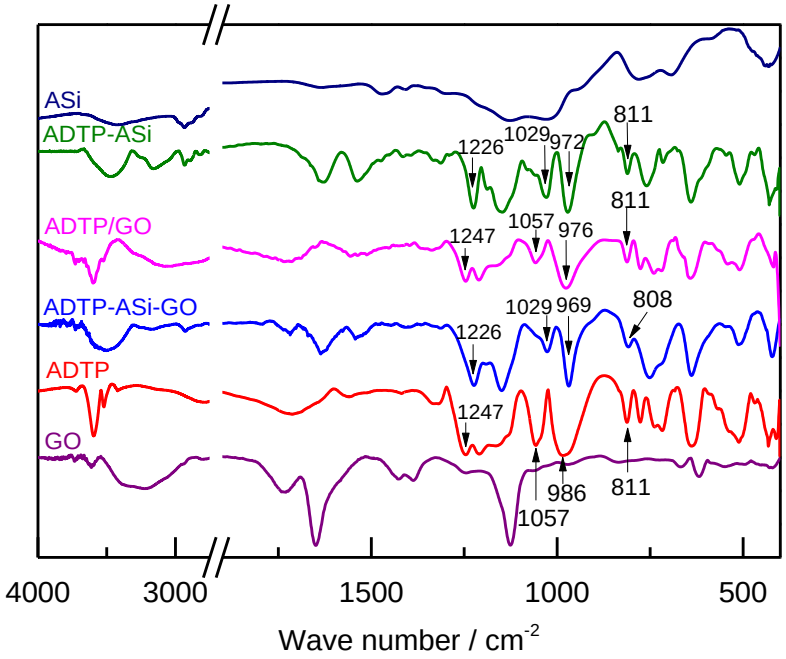


**Figure 5.** FTIR spectra of GO, ADTP, ASi, ADTP-ASi, ADTP-GO hybrid, and ADTP/GO blend

FTIR spectra of GO and ADTP-GO are also presented in Figure 5. The characteristic absorption bands of GO were observed at 1120cm$^{-1}$ (C-O-C), 1220cm$^{-1}$ (C-O), 1625cm$^{-1}$ (C=C), 1741cm$^{-1}$ (C=O), 3447cm$^{-1}$ (-OH), which exhibited a large number of oxygen-containing functional groups (such as a hydroxyl, a carboxyl and epoxide group) in GO.

For the spectrum of ADTP-GO hybrid, the peak at 1035cm$^{-1}$ representing the interatomic vibration band of the Si-O-Si bond, the peak at 1115cm$^{-1}$ representing the symmetrical stretching vibration band of Si-O-C bond. The absorption peak at 747cm$^{-1}$ representing the bending vibration band of the Si-O-Al bond, indicating that the ASi was successfully modified on ADTP through chemical bonding. The peaks at 810cm$^{-1}$ and 1545cm$^{-1}$ representing the in-plane bending vibration band and out- of-plane bending vibration band of -NH bond, indicating that the chemical bonding between ASi and GO had existed. The appearance of the peaks due to Si-O-Al and -NH demonstrated that ADTP and GO nano-sheets were bonded with ASi.

**Morphology of Composite Pigments.** The morphologies of ADTP, ADTP-ASi and ADTP-GO hybrid were investigated by using SEM technology as shown in Figure 6. Figure 6a shows the SEM image of ADTP lamellar particles with sharp edges. Figure 6b shows a stripped crystal structure of ADTP-ASi. Figure 6c demonstrates indistinct shapes of ADTP lamellar structure with GO sheets spreading over it in ADTP-GO hybrid. Figure 6d is high magnification SEM image of the hybrid.

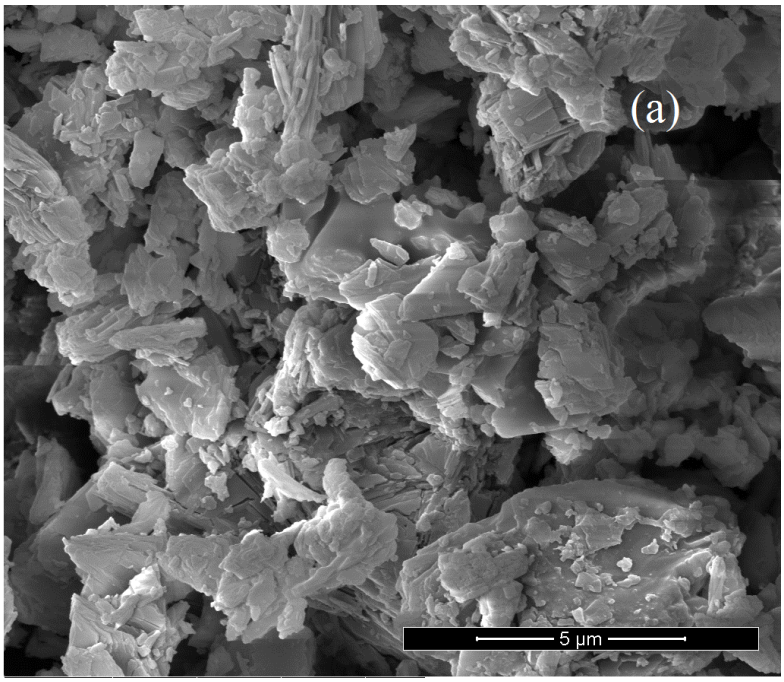
(a)
5 µm

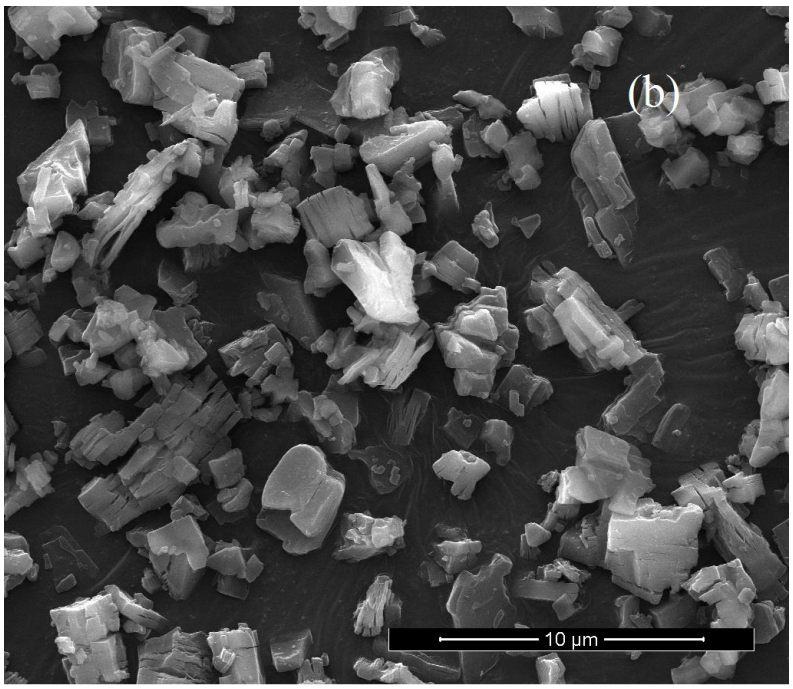
(b)
10 µm

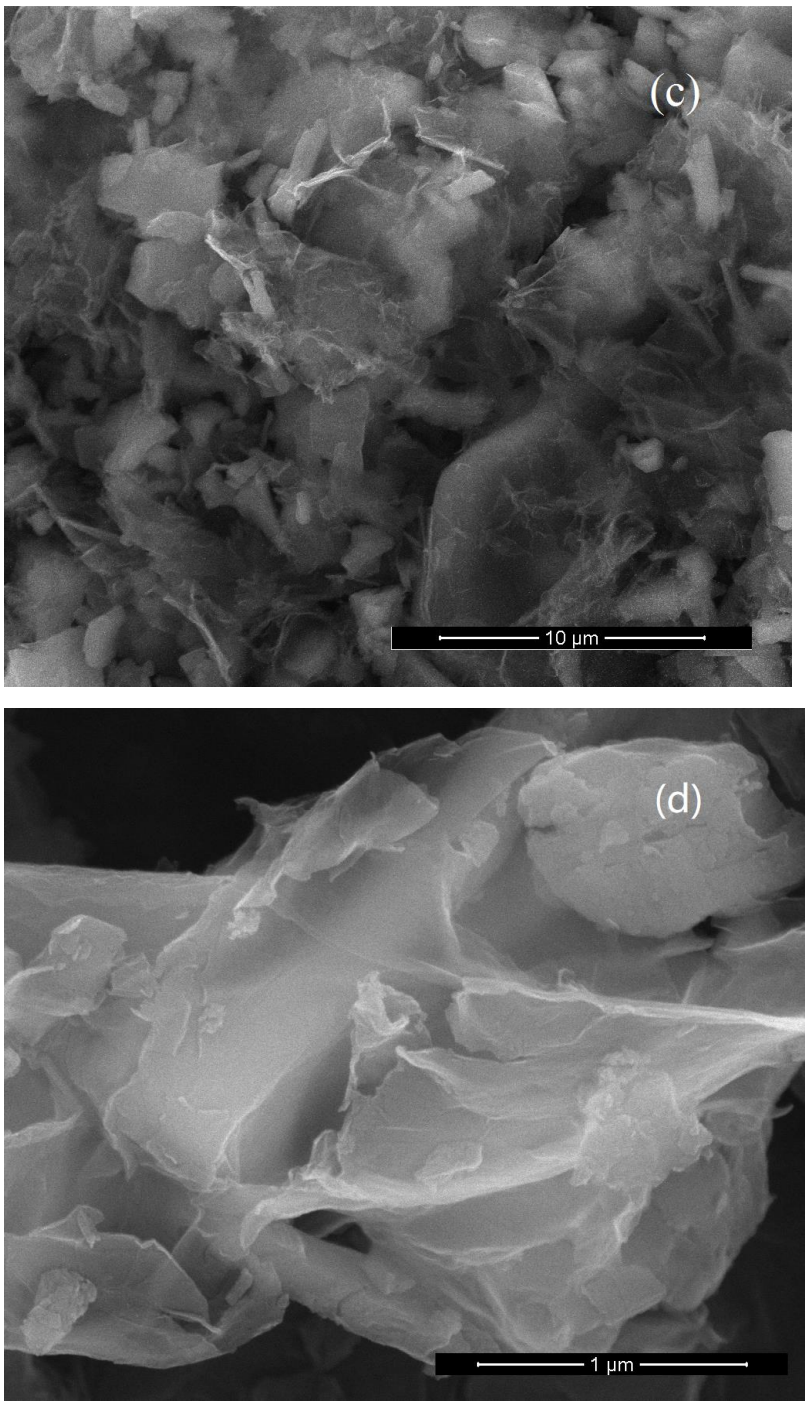


**Figure 6.** SEM morphologies of ADTP(a), ADTP-ASi (b) and ADTP-GO (c and d)

In Figure 6d, it is clear that ADTP and GO are combined by overlay and encapsulation in ADTP-GO hybrid, which indicated a three-dimensional interaction. There should be two kinds of driving forces for GO to be combined with ADTP in the hybrid. One is the connection of ASi coupling agent, the other is the strong interaction between the surface groups of ADTP and GO, such as the formation of hydrogen bonds.

**Electrochemical Polarization Analysis.** The corrosion inhibitions of epoxy coatings pigmented by ADTP, GO, ADTP/GO blend, and ADTP-GO hybrid were considered by electrochemical methods. Electrochemical measurements were conducted to study the anticorrosion behaviors of the aforementioned pigment types in epoxy coatings applied on mild steel exposed to

3.5% NaCl aqueous solution.

Corrosion potential and corrosion current can connect the fundamental electrochemistry and the practical corrosion behavior of metals. The value of the corrosion potential indicates the state of a corroding metal while that of the corrosion current reflects the instantaneous corrosion rate at the time of measurement.[23] With the measurement of corrosion potential and corrosion current, the protection ability of coatings on metals can be evaluated. In this study, Tafel polarization measurement was used to deduce corrosion potential and corrosion current. Figure 7 shows typical polarization curves after exposure of 48 hours to 3.5 wt.% NaCl solution. The corrosion potential ($E_{corr}$) and the corrosion current density ($i_{corr}$) were deduced from Tafel plots by extrapolating the linear portions of the curves. The obtained parameters via exposure time are shown in Figure 8 and Figure 9. The curves in Figure 8 describe the evolution of $E_{corr}$ of the coated mild steel substrates with time during exposure, and the curves in Figure 9 show $i_{corr}$ at the corresponding $E_{corr}$.

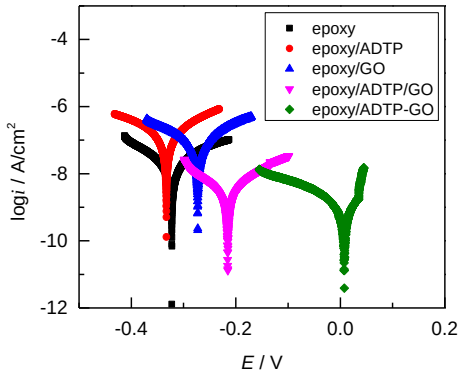


**Figure 7.** Typical polarization plots for mild steel substrate coated by pure epoxy, epoxy/ADTP, epoxy/GO, epoxy/ADTP/GO, and epoxy/ADTP-GO coatings after exposure of 48 hours to 3.5wt.% NaCl solution.

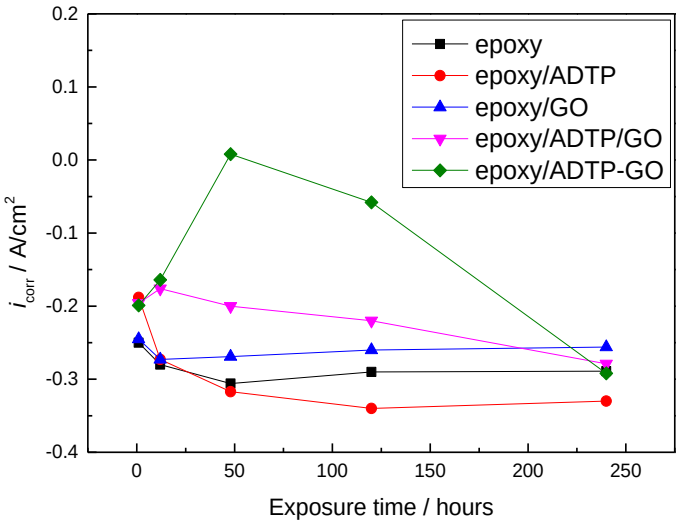


**Figure 8.** Polarization parameter $E_{corr}$ obtained by the Tafel extrapolation method.

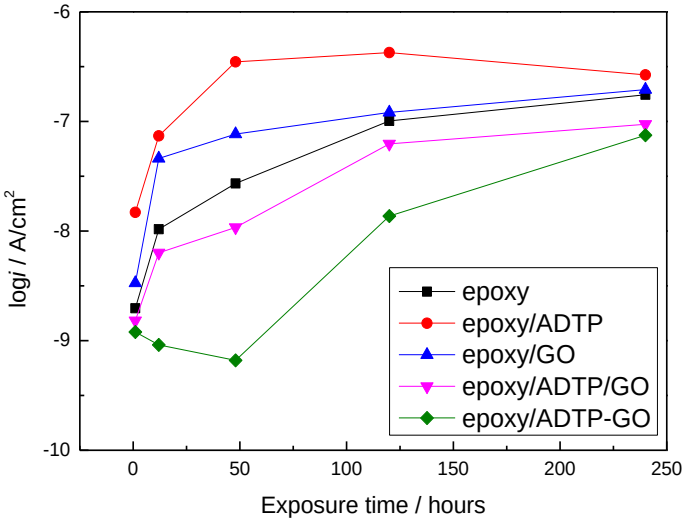


**Figure 9.** Polarization parameter $i_{corr}$ obtained by the Tafel extrapolation method.

Corrosion potential is a mixed potential (also an open-circuit potential or rest potential) at which the rate of anodic dissolution of the electrode equals the rate of cathodic reactions and there is no net current flowing in or out of the electrode. Corrosion current is the dissolution current at the corrosion potential.[23] A positive shift of the corrosion potential indicates an increase in the corrosion resistance, and a decrease of corrosion current means a decline in corrosion rate.

In the early-term of exposure, $E_{corr}$ and $i_{corr}$ for epoxy/ADTP-GO coating increased and decreased, respectively, which showed that epoxy/ADTP-GO coating possessed better anti-corrosion ability than other tested coatings. By contrast, other coatings exhibited significantly higher $i_{corr}$ and more negative $E_{corr}$ throughout the testing period as shown in Figure 8 and Figure 9, indicating a fast corrosion rate. The good protective performance of epoxy/ADTP-GO coating should be attributed to the synergistic effect of ADTP and GO in the coating.

**EIS Analysis.** EIS technique was used to evaluate the synergistic effect of GO nanosheets and ADTP on electrochemical properties and corrosion inhibition of epoxy coatings. The Bode and Nyquist plots of mild steel substrate coated by pure epoxy, epoxy/ADTP, epoxy/GO, epoxy/ADTP/GO and epoxy/ADTP-GO coatings exposed to 3.5wt.% NaCl solution after 1, 12, 48 and 240 hours are shown in Figure 10. It can be clearly observed in Figure 10a, c, e and g that the Z module plots for all samples descended with increasing exposure time, indicating the decrease of corrosion inhibition. In case of pure epoxy coating after 1 hour of exposure (Figure 10b), the control step of electrode process was electrochemical reaction, indicating that corrosive species had penetrated pure epoxy coating and reached the coating/substrate interface, causing the decrease of electro-resistance and the beginning of electrochemical corrosion at the coatings/metal interface. As for other samples, corrosive pitting occurred after 1 hour of exposure. In Figure 10d, f and h, the oblique line of Warburg impedance appeared, and indicated that the electrode process was controlled by corrosive species diffusing. The presence of Warburg impedance indicated that non-interconnected porous structure had been formed, and the diffusion process had dominated corrosion at low frequencies for all samples after 12 hours of exposure.

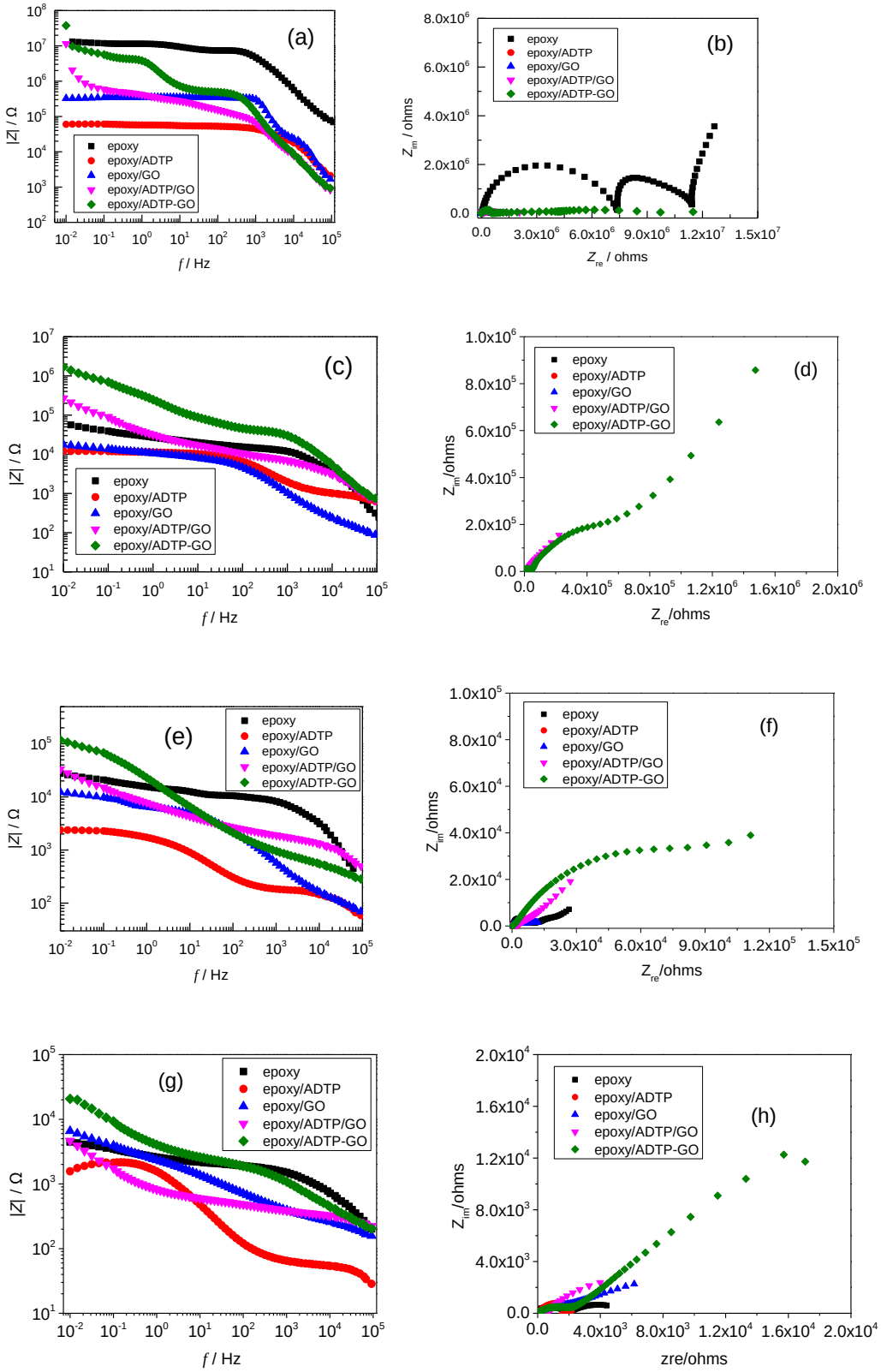


**Figure 10.** Bode plots (a, c, e and g) and Nyquist plots (b, d, f and h) for pure epoxy, epoxy/ADTP, epoxy/GO, epoxy/ADTP/GO, and epoxy/ADTP-GO coatings on mild steel substrates exposed to 3.5 wt. % NaCl solution for 1 hour (a and b), 12 hours (c and d), 48 hours (e and f), and 240 hours (g and h).

The variation in the Z module value at low frequency of 0.01Hz ($|Z|_{0.01Hz}$) for different samples during exposure is presented in Figure 11. As shown, the $|Z|_{0.01Hz}$ value for pure epoxy and epoxy/ADTP/GO coatings decreased significantly in the early immersion stage and slightly in the following immersion stage. This significant decrease was due to diffusion of corrosive agents through porous structure of epoxy coating and delamination of coating from substrate surface. The slight decrease indicated that corrosion products had been formed and filled the pores in the coating. In case of epoxy/ADTP-GO coating, gradual decreasing trend of the $|Z|_{0.01Hz}$ value are observed in Figure 11. The trend was due to blocked continuous diffusion of species through coatings.

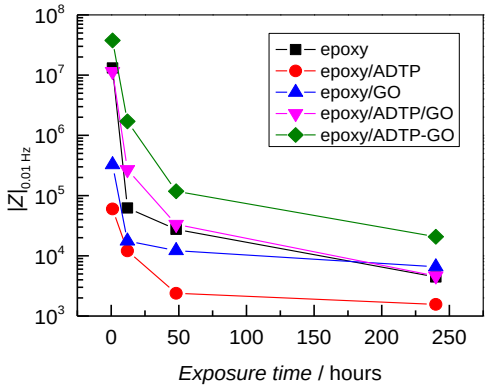


**Figure 11.** |Z| at 0.01Hz after 12 hours of exposure to 3.5wt.% NaCl solution.

In order to further explore the difference between epoxy coatings containing different pigments, the experimental EIS data were fitted with appropriate electrochemical equivalent circuits. In fact, the failure process of coatings was very complex, and the coatings did not show the same performance during the failure process. Additionally, the environment and the protected matrix of coatings were constantly changing. Therefore, new resistor-capacitance (*RC*) circuits continuously appeared and contributed impedance to the whole electrochemical system, and the equivalent circuits needed to be repaired in time. After 48 hours of exposure to 3.5wt.% NaCl solution, the corrosion species had reached the interface between the coating and the steel substrate, so the equivalent circuit was almost the same with further exposure to the NaCl solution. The EIS data after 48 hours of exposure were analyzed and fitted by a ZSimpWin equivalent circuit fitting software and the fitting electric circuits are shown in Figure 12.

The proposed equivalent circuits consist of solution resistance ($R_s$), coating constant phase element ($C_c$), coating resistance ($R_c$), pore resistance ($R_p$), double layer constant phase element ($C_{dl}$), charge transfer resistance ($R_{ct}$), and Warburg impedance element ($W$). Figure 12a preferably fitted EIS data of pure epoxy and epoxy/GO coatings, and Figure 12b EIS data of epoxy/ADTP/GO and epoxy/ADTP-GO coatings. The impedance spectra of Figure 12c were in good agreement with EIS data of epoxy/ADTP coating. At a glance, Figure 12b is a combination of Figure 12a and c. The combination of electric circuits resulted from several electrochemical processes. By comparison, *W* impedance is in the equivalent circuit of Figure 12c, but not in Figure 12a and b. This *RC* element described mass transport processes through a diffusion layer, so the presence of *W* in Figure 12a for epoxy/GO coating and Figure 12b for epoxy/ADTP/GO and epoxy/ADTP-GO coatings was attributed to GO physical obstruction against transport of corrosion species through the coating layers.

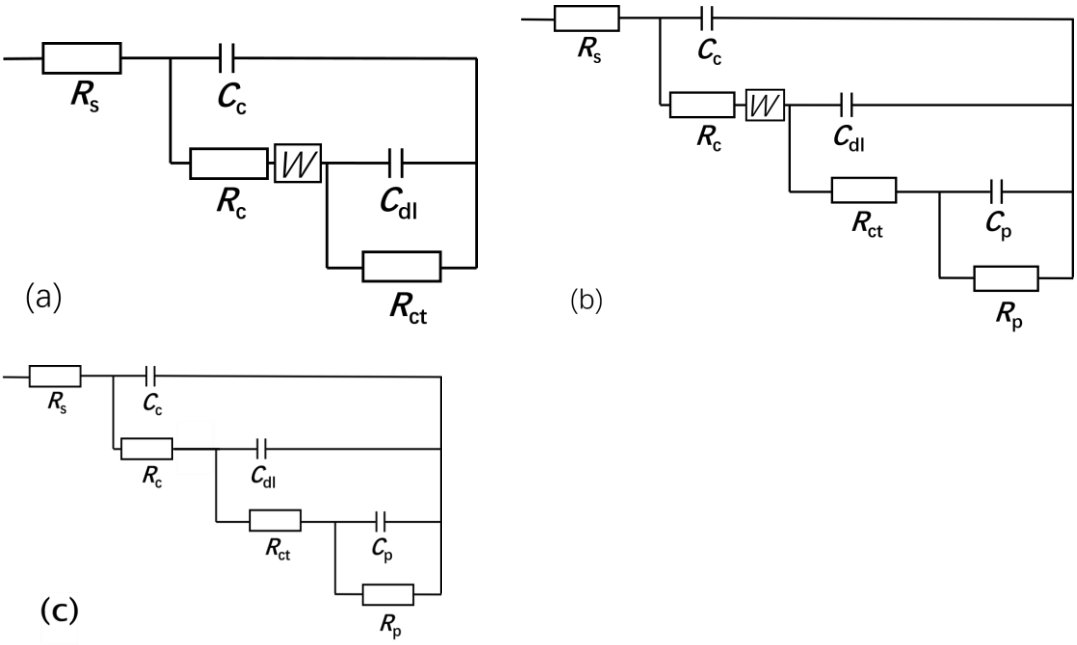


**Figure 12.** Equivalent circuit model for numerical simulation of EIS data after exposure to 3.5wt.% NaCl solution for 48 hours.

The fitting electrochemical parameters are listed in Table 1. As the electric resistance of coating against transfer of ions through pores in coating, $R_c$ illustrated coating porosity and degradation. It seems that there was less porosity in pure epoxy coating. Additionally, $R_{ct}$ evaluated the electric resistance against electron transfer at metal/coating interface and was related to corrosion rate. The value of $R_{ct}$ in Table 1 appeared to be an acknowledgment that the corrosion rate for epoxy/ADTP-GO coating was lower than that for epoxy/ADTP/GO. Especially, the values of $W$ for epoxy coatings pigmented by GO, ADTP/GO and ADTP-GO are higher than that for pure epoxy coating, which indicated a weak obstruction ability of the protective layer of pure epoxy coating.

**Table 1**. Electrochemical corrosion parameters of pure epoxy, epoxy/ADTP, epoxy/GO, epoxy/ADTP/GO and epoxy/ADTP-GO coatings fitted from the equivalent circuit after 48 hours of exposure [a]

| Parameter | pure epoxy | epoxy/ADTP | epoxy/GO | epoxy/ADTP/GO | epoxy/ADTP-GO |
|---|---|---|---|---|---|
| $C_c$, $\times10^{-10}$ $S^n/cm^2$ | 4.53 | 22.9 | 22.0 | 2.68 | 4.08 |
| $n_1$ | 1 | 1 | 1 | 1 | 1 |
| $R_c$, $\times10^4\Omega$ | 7.99 | 0.2 | 0.181 | 1.48 | 0.878 |
| $W$, $\times10^{-7}$ $S^{1/2}/cm^2$ | 2.71 | | 411 | 134 | 137 |
| $C_{dl}$, $\times10^{-10}$ $S^n/cm^2$ | 3.84 | 6381 | 7573 | 34.8 | 2200 |
| $n_2$ | 1 | 0.714 | 0.6657 | 1 | 0.576 |
| $R_{ct}$, $\times10^5\Omega$ | 5.05 | 0.09 | 0.786 | 1.08 | 3.99 |
| $C_p$, $\times10^{-7}$ $S^n/cm^2$ | | 47.3 | | 1.47 | 38.3 |
| $n_3$ | | 0.777 | | 0.396 | 0.584 |
| $R_p$, $\times10^5\Omega$ | | 0.145 | | 1.05 | 12.5 |

[a] Entries are average values, N = 3.

**Morphology.** Further, in order to investigate the synergetic effect of ADTP and GO in ADTP/GO blend and ADTP-GO hybrid, the fracture surfaces of the cured epoxy coatings detached

from the mild steel substrate were observed by SEM. The SEM images of fracture surfaces are shown in Figure 13. As shown in Figure 13a, ADTP particles are large and aggregated in the epoxy/ADTP coating. Comparatively speaking, ADTP particles in epoxy/ADTP/GO and epoxy/ADTP-GO coatings preserved good dispersity and uniformity as shown in Figure 13b and c, which can be attributed to synergistic effect of ADTP and GO.

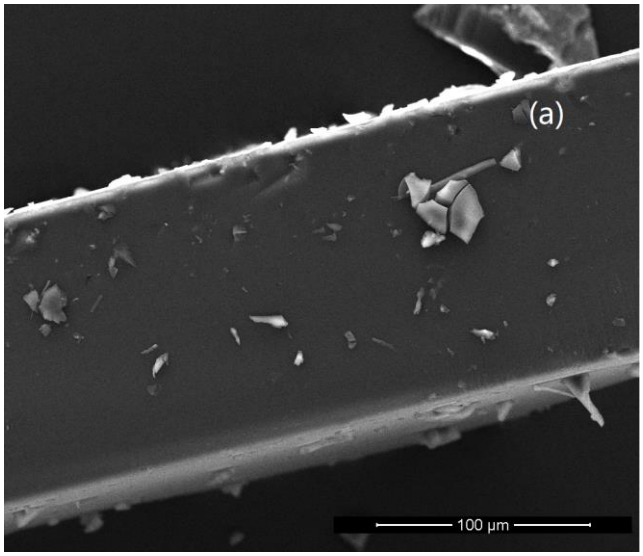


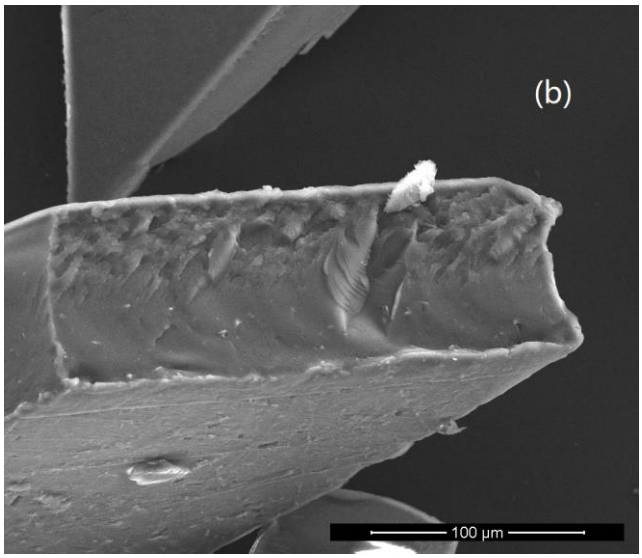

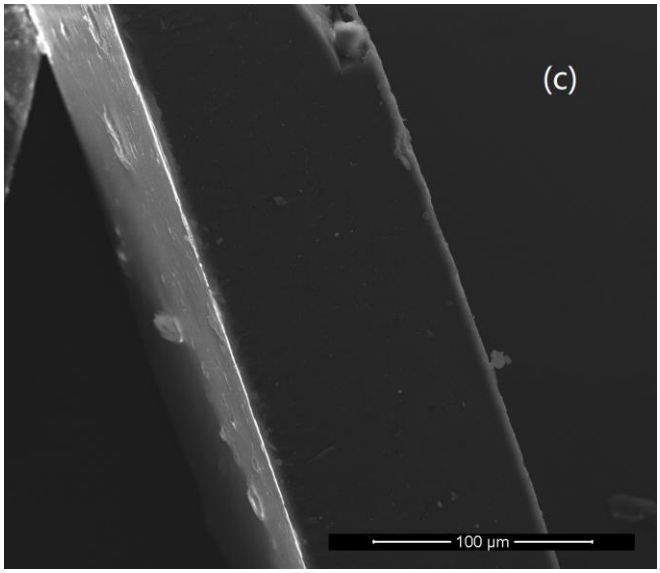


**Figure 13.** SEM micrographs of fracture surfaces of (a) epoxy/ADTP, (b) epoxy/ADTP/GO, (c) epoxy/ADTP-GO coatings

## ■ CONCLUSION

ADTP and GO were combined in two approaches, i.e., chemical coupling (ADTP-GO hybrid) and physical blending (ADTP/GO blend). The former was prepared by using ASi coupling method, and the later by mechanically mixing. ADTP and GO displayed synergistic effect in promoting dispersion in both of epoxy/ADTP-GO and epoxy/ADTP/GO coatings. However, in terms of anti-corrosion performance, there was no significant synergistic effect between ADTP and GO in epoxy/ADTP/GO coating. Comparison indicated that ADTP-GO hybrid had a stronger blocking ability to corrosive species passing through the coating layer and displayed an obvious advantage in improving the corrosion inhibition performance of waterborne epoxy coating at a low content (2 wt.%). Although weaker than epoxy/ADTP-GO coating, epoxy/ADTP/GO coating was better that pure epoxy, epoxy/ADTP, and epoxy/GO coatings in anti-corrosion performance. It seems that the combination of A and B produced synergistic effect, and the synergistic effect was more obvious after chemical coupling.

## ■ Author information

**Corresponding Author**

*Tel: +86 18623719057, +86 371 67758729. E-mail: weiqiang_song@haut.edu.cn.

**ORCID**

Weiqiang Song: 0000-0003-4811-5766

**Acknowledgments**

This work was supported by Science and Education Integration Project of Henan University of Technology in 2018 (Grant no. 34)

***No conflict of interest exits in the submission of this manuscript.***

**References**

(1) Gray, J. E., Luan, B. Protective coatings on magnesium and its alloys - a critical review. *Cheminform.* **2002**, *336*, 88.

(2) Rahman, O. U., Kashif, M., Ahmad, S. Nanoferrite dispersed Waterborne epoxy-acrylate: anticorrosive nanocomposite coatings. *Prog. Org. Coat.* **2015**, *80*, 77.
(3) Zhan, Y., Zhang, J., Wan, X, Long, Z., He, S., He, Y. Epoxy composites coating with $Fe_3O_4$ decorated graphene oxide: Modified bio-inspired surface chemistry, synergistic effect and improved anti-corrosion performance. *Appl. Surf. Sci.* **2018**, *436*, 756.
(4) Tomoi, M. Toughening of Epoxy Resins. *Des. Monomers Polym.* **2006**, *9*, 129.
(5) Xu, Z. P., Han, W. L., Zhang, Y. Y., Xie, B. B. Study on epoxy coating which could be applied on high temperature (70°C) steel surface. *Appl. Mech. Mater.* **2012**, *159*, 311.
(6) Bera, S., Rout, T. K., Udayabhanu, G., Narayan, R. S. F. Water-based & eco-friendly epoxy-silane hybrid coating for enhanced corrosion protection & adhesion on galvanized steel. *Prog. Org. Coat.* **2016**, *101*, 24.
(7) Zhu, Y. X., Duan, C. Y., Liu, H. Y., Chen, Y. F., Wang, Y. Graphene coating for anti-corrosion and the investigation of failure mechanism. *J. Phys. D: Appl. Phys.* **2017**, **50**, 114001.
(8) Ramezanzadeh, B., Niroumandrad, S., Ahmadi, A., Mahdavian, M., Moghadam, M. H. M. Enhancement of barrier and corrosion protection performance of an epoxy coating through wet transfer of amino functionalized graphene oxide. *Corros. Sci.* **2016**, *103*, 283.
(9) Madhankumar, A., Nagarajan, S., Rajendran, N., Nishimura, T. Effect of Si nanoparticles on the corrosion protection performance of organic coating on carbon steel in chloride environment. *Met. Mater. Int.* **2012**, *18*, 96.
(10) Zhang, X. L., Zhang, S. L., Lei, Y. Corrosion resistance of in-situ phosphatizing organic coating modified with rare earth oxide nanoparticles. *Met. Finish.* **2012**, *110*, 24.
(11) Richards, C. A. J., Glover, C. F., Williams, G., Mcmurray, H. N., Baker, J. Evaluation of multi-layered graphene nano-platelet composite coatings for corrosion control part I-Contact potentials and gas permeability. *Corros. Sci.* **2018**, *136*, 285
(12) Dhirde, P. G., Chada, V. G. R., Mallik, B. P., Moitra, N. Alkyd-clay nanocomposites for improved anticorrosion and mechanical performance of coating. *Polym. Compos.* **2018**, *39*, 2922.
(13) Rui, D., Li, W. A brief introduction to corrosion protective films and coatings based on graphene and graphene oxide. *J. Alloy. Compd.* **2018**, *764*,1039.
(14) Rui, D., Yan, Z., Yu, H., Li, W., Wang, X., Gui, T. Study of water permeation dynamics and anti-corrosion mechanism of graphene/zinc coatings. *J. Alloy. Compd.* **2018**, *748*, 481.
(15) Nayak, S. R., Mohana, K. N. S. Corrosion protection performance of functionalized graphene oxide nanocomposite coating on mild steel. *Surfaces and Interfaces* **2018**, *11*, 63.
(16) Sørensen, P. A., Kiil, S., Dam-Johansen, K., Weinell, C. E. Anticorrosive coatings: a review. *J. Coat. Tech. Res.* **2009**, *6*, 135.
(17) Song, W., Yang, L., Ma, X., Liang, G. Effects of CaO and MgO on Anticorrosive Performance of Aluminum Dihydrogen Tripolyphosphate on Mild Steel. *Ind. Eng. Chem. Res.* **2018**, *57*, 13578.
(18) Dodds, P. C., Williams, G., Radcliffe, J. Chromate-free smart release corrosion inhibitive pigments containing cations. *Prog. Org. Coat.* **2017**, *102*, Part A, 107.
(19) Gao, F., Xu, C., Hu, H., Wang, Q., Gao, Y., Chen, H., Guo, Q., Chen, D., Eder, D. Biomimetic synthesis and characterization of hydroxyapatite/graphene oxide hybrid coating on mg alloy with enhanced corrosion resistance. *Mater. Lett.* **2015**, *138*, 25.
(20) Nguyen, T. D., Tran, B. A., Vu, K. O., Nguyen, A. S., Trinh, A. T., Pham, G. V., Hang, T. X. Corrosion protection of carbon steel using hydrotalcite/graphene oxide nanohybrid. *J. Coat. Technol. Res.* **2018**,

(21) Zhan, Y., Zhang, J., Wan, X., Long, Z., He, S., He, Y. Epoxy composites coating with $Fe_3O_4$ decorated graphene oxide: modified bio-inspired surface chemistry, synergistic effect and improved anti-corrosion performance. *Appl. Surf. Sci.* **2018**, *436*, 756.
(22) Marsh, T. P. Studies into the ion exchange and intercalation properties of AlH2P3O10·2H2O. University of Birmingham, Birmingham, UK, 2011.
(23) Zhang X.G. Corrosion Potential and Corrosion Current. In: Corrosion and Electrochemistry of Zinc. Springer, Boston, MA, 1996.